



The Increase of the Reactivity of Molecular Hydrogen with Hydroxyl Radical from the Gas Phase versus an Aqueous Environment: Quantum Chemistry and Transition State-Theory Calculations

Valter H. Carvalho-Silva^{1(✉)}, Eduardo C. Vaz^{1,2},
Nayara D. Coutinho², Hikaru Kobayashi³, Yuki Kobayashi³,
Toshio Kasai^{3,4}, Federico Palazzetti², Andrea Lombardi²,
and Vincenzo Aquilanti^{2,5}

¹ Grupo de Química Teórica e Estrutural de Anápolis,
Ciências Exatas e Tecnológicas, Universidade Estadual de Goiás,
CP 459, Anápolis, GO 75001-970, Brazil

fatioleg@gmail.com

² Dipartimento di Chimica, Biologia e Biotecnologie, Università di Perugia,
Via Elce di Sotto 8, 06123 Perugia, Italy

³ The Institute of Scientific and Industrial Research, Osaka University,
8-1 Mihogaoka, Osaka, Ibaraki 567-0047, Japan

⁴ Department of Chemistry, National Taiwan University, Taipei 10617, Taiwan

⁵ Istituto di Struttura della Materia, Consiglio Nazionale delle Ricerche,
00185 Rome, Italy

Abstract. One of the simplest elementary reactions, that between H_2 and OH , is of great theoretical interest in chemical kinetics. Surprisingly it turned out recently to be of importance in medical and biological environments, in search of role of hydrogen as radical scavenger participating in the human body: water is supposed to be of possible influence in this reaction. However, there are no theoretical studies considering solvent effects in the title reaction which in the gas phase is slow. Here, we aim to analyze the $H_2 + OH$ reaction with a blend of electronic structure calculations and the *deformed* Transition-State Theory (*d*-TST) approach. Inclusion of the continuum solvation model density (SMD) was applied for mimicking the role of the aqueous phase. Preliminary results demonstrate an enormous increase in the reactivity between H_2 and OH molecules in water environment, approximately 150- and 138-fold at 25 °C and 36.5 °C, respectively. We expect that these results can help to shed new light on the understanding of the $H_2 + OH$ reaction in aqueous phase, paving the way to research for medical and technological applications.

1 Introduction

The reaction between H_2 and OH molecules is being demonstrated to be of great importance in biological and medical [1] environments, in spite of the simplicity of the molecules participating in the process. The H_2 molecule is the smallest gas molecule

composed of two protons and two electrons, forming a very stable compound that reacts with the oxide radical ion (O^-) [2]. There are several documentations regarding the antioxidant performance of the H_2 molecule. Studies of selectivity of H_2 molecule in cells inducing oxidative stress and reducing cytotoxicity reactive of oxygenated species, *i.e.*, hydroxyl radical [2–4]. Due to the applicability on the human body, water is supposed to be of great influence in this reaction, however, there are scarce studies from a theoretical viewpoint [5].

The four-body reaction investigation has been propitiated a deep understanding of the mechanism and reactivity of chemical reactions in the gas phase [6–9]. Recently, the prototypical $H_2 + OH$ reaction has been highlighted due to the publication of a paper by Ohsawa et al. [4], which presented results with a significant reduction of cerebral infarction in rats when exposed to of 2% to 4% v/v of molecular hydrogen mixtures. Later works [2, 3, 5, 10–16] obtained promising results in the treatment of 63 types of diseases with the administration of H_2 in several medical areas. The efficacy of the hydrogen molecule was suggested due to neutralization of OH radical [17], in a few cases prejudicial to a living organism, which H_2 has reactive specificity [4]. Concomitantly, this reaction came out to be important in other applications, such as the control of free radicals in the atmosphere [18], gas- and condensed phase reactions [19–21] and photosensitive materials [22]. On another context, the $H_2 + OH$ reaction has been mainly exploited to redirect H_2 gases from nuclear power plants to be reformed. Molecular hydrogen (H_2) has been playing a key role in nuclear power plants since water is used in the refrigeration of reactors with consequent high concentration H_2 and hydrogen peroxide (H_2O_2) formation due water radiolysis – interaction with alpha, beta and gamma radiation [23–25]. The high concentration of these generated gases is a concern to avoid explosive conditions since the water radiolysis under extreme conditions is not fully understood due to the rich and inherent complexity of chemical activity [26].

There is extensive experimental and theoretical rate constant investigation of the title reaction [5] and, due to its importance, many potential energy surfaces (PES) have been proposed to estimate theoretically thermodynamic and kinetic parameters. Chen et al. [27] proposed recently a global PES using neural networks method based on approximately 17,000 *ab initio* energies calculated via UCCSD(T)-F12a/AVTZ. Additionally, quantum-classical (QC) investigations reported the connection of the reactivity of H_2 with vibrational excitation energy exchange while OH radicals are not affected [28]. Recently, Kastner et al. [20] obtained theoretical reaction rate constant, in the range of the 150 K to 1000 K, with excellent agreement with experimental data. Talukdar et al. [29] and Bhattacharya et al. [6] demonstrated the presence of an isotopic effect in the reaction involving molecular hydrogen - especially in low-temperature conditions – a classical signature of quantum tunneling effect [6, 29].

Here, the $H_2 + OH$ reaction in the gas-phase and in the aqueous environments (due relevance in living organism previously described) has been investigated with a blend of electronic structure calculations - Quadratic Configuration Interaction involving single, double and triple substitutions excitations QCISD(T), with the *deformed*

Transition-State Theory (*d*-TST) to account for the tunneling effect. A similar approach was previously developed and illustrated by our group in various cases of four-body reactions, with promising results suggesting a significant role of stereodynamics, roaming and quantum effects in influencing the rates of reactive [18, 20, 30–32], so qualifying our theoretical tools to cope with this reaction.

2 Computational Procedures

2.1 Stationary Electronic Structure Calculations

The electronic structure properties of the reactants, the products, and the transition state were calculated employing the Møller-Plesset [33], Configuration Interaction [34], in combination with 6-311++G(3df,3pd) and aug-cc-pVDZ basis set. The specific level of calculation was selected to perform analyses and comparison with experimental data: CISD(T)/aug-cc-pVDZ//MP2/6-311+G(3df,2pd). The stationary points were characterized by analytic harmonic frequency calculations. The absence or existence of one imaginary frequency for crossing the barrier characterizes the optimized structures as local minimum or transition state, respectively. The zero-point vibrational energy contributions were considered in the calculation of the barrier. To account for the solvent effect the continuum solvation model density was applied to mimicking the water ambience (SMD) [35].

2.2 Reaction Rate Theories

The reaction rate constants (*k*) were calculated by deformed-transition state theory (*d*-TST). This phenomenological formulation covers cases of concave deviation from Arrhenius law against the reciprocal of temperatures for elementary chemical reactions, exhibiting *sub*-Arrhenius behavior. In general, this behavior is a signature of quantum tunneling. To account the quantum tunneling in chemical reactions in the *deformed* formulation, *d* parameter is introduced from transitivity concept γ [36, 37] namely the inverse of activation energy ($1/E_a$) with reciprocal of the temperature (β) truncated at an order higher than one:

$$\gamma \equiv \frac{1}{E_a} = \frac{1}{\varepsilon^\ddagger} - d\beta \quad (1)$$

where ε^\ddagger is a constant and represents an energetic obstacle to the reaction at high temperatures and $\beta = 1/k_B T$, where k_B is Boltzmann's constant and T is the absolute temperature. In Ref. [38], an explicit procedure for calculation of *d* was developed as inversely proportional to the square of the barrier (ε^\ddagger) and directly proportional to the

square of the frequency for crossing the barrier (v^\ddagger) at maximum in the minimum energy path on the potential energy surface,

$$d = -\frac{1}{3} \left(\frac{hv^\ddagger}{2\varepsilon^\ddagger} \right)^2 \quad (2)$$

where h is Planck's constant.

The tunneling corrected averaged by Boltzmann factor from TST formulation was replaced by the deformed exponential function, yielding the d -TST formulation [39]

$$k(\beta) = \frac{1}{h\beta} \frac{Q^\ddagger}{Q_{Reac}} \left(1 - d\varepsilon^\ddagger\beta \right)^{1/d} \quad (3)$$

where Q_{Reac} and Q^\ddagger are the partition function (translational, vibrational, rotational and electronic contributions) of the reactants and of the activated complex, respectively. Equation (4) recovers the TST rate constant when d tends to zero, due to the Euler limit, $\lim_{d \rightarrow 0} \left(1 - d\varepsilon^\ddagger\beta \right)^{1/d} = e^{-\varepsilon^\ddagger\beta}$.

The tunneling regime can be characterized considering the crossover temperature parameter $T_c = hv^\ddagger/2\pi k_B$ [40, 41], conventionally establishing (within some arbitrariness) the ranges of the regimes for a specific imaginary frequency at the top of the barrier point, v^\ddagger : negligible ($4T_c > T > 2T_c$), moderate ($2T_c > T > T_c$) and deep ($T_c > T$) regimes.

A phenomenological representation for the temperature dependence of obtained rate constants to cover the regimes, except at deep tunneling, can be obtained by Aquilanti-Mundim deformed Arrhenius formula (AM) [42]

$$k(\beta) = A(1 - \bar{d}E_0\beta)^{1/\bar{d}} \quad (4)$$

A and \bar{d} are the pre-exponential factor and the deformed parameter, respectively. [Note a change in the notation here, needed in order to avoid ambiguities: in terms of the fitted equation, we defined \bar{d} which is different from d and E_0 which is different from ε^\ddagger .

All kinetic and associated parameters were calculated with the Transitivity Code-version 1.0.0: details of the computational program can be found on the www.vhcsgroup.com/transitivity web page.

3 Results and Discussion

Table 1 shows theoretical imaginary vibrational frequency (cm^{-1}), crossover temperature and relative energies (in kcal mol^{-1}) of the stationary points along the $\text{H}_2 + \text{OH} \rightarrow \text{H}_2\text{O} + \text{H}$ reaction coordinate at carefully chosen different levels of

theory. The transition state in gas-phase presents an imaginary vibrational frequency of $1531i$ at MP2/6-311++G(3df,3pd), clearly different from the result obtained by Meisner and Kastner (1199*i*) at CCSD(T)-F12/cc-pVDZ-F12. Consequently, a difference around 100 K is observed for crossover temperature. This difference suggests an improvement in our calculation, which was performed only in energy at CISD(T)/aug-cc-pVDZ//MP2/6-311+G(3df,2pd) level.

Table 1. Imaginary vibrational frequencies (ν^\ddagger) in cm^{-1} , cross over temperature (T_c) in Kelvin, the barrier height (ϵ^\ddagger) and exothermicity-type energies in kcal.mol^{-1} for OH + H₂ reaction both gas- and aqueous-phase. Theoretical data are also presented for comparison.

	ν^\ddagger	T_c	ϵ^\ddagger	ΔE
Gas-phase [MP2]	1531 <i>i</i>	350	8.05	-22.97
Gas-phase [CISD(T)//MP2]	–		6.63	-14.30
Aqueous-phase [CISD(T)//MP2]	–		6.27	-16.71
Meisner and Kastner (Gas phase) [20]	1199 <i>i</i>	270	5.38	-16.27

Table 1 also present barrier height calculated at MP2 level of theory in gas-phase, around 8 kcal.mol^{-1} , different from Meisner and Kastner obtained with coupled cluster level of calculation. However, our calculation yields a significant decrease in barrier energy and in exothermicity values at CISD(T)/aug-cc-pVDZ//MP2/6-311+G(3df,2pd) level with a reasonable agreement with Meisner and Kastner [20]. To account for the solvent effect, the continuum solvation model density was applied for mimicking the aqueous-phase (SMD) at CISD(T)/aug-cc-pVDZ//MP2/6-311+G(3df,2pd) level of calculation. Comparison between gas- and aqueous-phase presents a slight decrease in the barrier height at the similar level of calculation.

We calculate the kinetic rate constant using deformed-Transition State Theory (*d*-TST) in a realistic range of temperature (250–350 K) at CISD(T)/aug-cc-pVDZ//MP2/6-311+G(3df,2pd) level of calculation for the title reaction in gas- and aqueous-phase. Figure 1 shows the comparison of the *d*-TST rate constant with previous theoretical [20, 43] and experimental [29, 30, 44–47] results for H₂ + OH → H₂O + H reaction: it is observed a slight difference with the literature in reaction rate constants in gas-phase, and an improvement in the reactivity with the inclusion of solvent effect. Here, we show experimental data of the reaction rate constants in aqueous-phase [48–50], and our preliminary calculations yield a reasonable qualitative agreement.

In this work, we use the AM formula, Eq. (4), to fit the temperature dependence of the reaction rate constants in gas- and aqueous-phase. AM formula has been successfully applied to a variety of chemical processes [42, 51–56]. The temperature dependence of the reaction rate constants can be expressed as

$$k_{Gas}(T) = 2.94 \times 10^{-10} \left(1 + \frac{459.40}{T} \right)^{-12.32}, \quad (5)$$

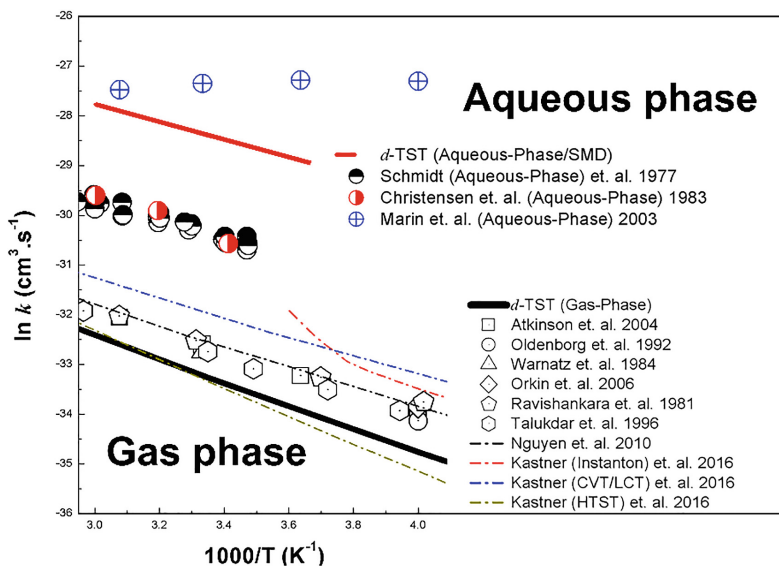


Fig. 1. Comparison of the *d*-TST rate constant with previous theoretical [20, 43] and experimental [29, 30, 44–47] results for $\text{H}_2 + \text{OH} \rightarrow +\text{H}_2\text{O} + \text{H}$ reaction.

and

$$k_{\text{Aqueous}}(T) = 1.64 \times 10^{-9} \left(1 + \frac{479.95}{T} \right)^{-8.55}. \quad (6)$$

The water environment produced a significant effect in the reactivity of the molecular hydrogen with hydroxyl radical as observed in Fig. 1. The reaction rate constants in aqueous-phase increase approximately 150- and 138-fold at 25 °C and 36.5 °C, respectively, see Eq. (7). The former temperature is conventionally used as the referential temperature in chemical reactions and the last mimics the human corporal temperature.

$$\frac{k_{\text{Aqueous}}(25\text{ °C})}{k_{\text{Gas}}(25\text{ °C})} \approx 150; \quad \frac{k_{\text{Aqueous}}(36.5\text{ °C})}{k_{\text{Gas}}(36.5\text{ °C})} \approx 138 \quad (7)$$

4 Conclusion

In summary, in this work we established the role of the aqueous environment for the $\text{OH} + \text{H}_2$ reaction based on high-level *deformed* Transition-State Theory. The following key findings emerged from our investigation and support the assumptions presented in this work:

- All the stationary points with the energetics and geometric parameters involved in the reaction were accurately characterized at the CISD(T)/aug-cc-pVDZ//MP2/6-311+G(3df,2pd) level of calculation.
- *Deformed* Transition-State Theory is shown to be suitable for describing the reaction rate constants in gas- and aqueous-phases.
- Water ambience produced a significant effect in the reactivity of the molecular hydrogen with hydroxyl radical, approximately 150- and 138-fold at 25 °C and 36.5 °C, respectively.

We expect that these results will pave the way to future studies for medical and technological applications.

Acknowledgments. VHCS thanks Brazilian agency CNPq for the research funding programs [Universal 01/2016 - Faixa A - 406063/2016-8] and Organizzazione Internazionale Italo-Latino Americana (ILLA) for Biotechnology Sector-2019 scholarship. VA, FP, AL acknowledge the Italian Ministry for Education, University and Research, MIUR, for financial support: SIR 2014 “Scientific Independence for young Researchers” (RBSI14U3VF). AL acknowledges the financial support from MIUR PRIN 2015 (contract 2015F59J3R 002).

References

1. Che, D.C., Shimouchi, A., Mizukami, T., Nose, K., Seiyama, A., Kasai, T.: Emanation of hydroxyl radicals from human skin. *IEEE Sens. J.* **13**, 1223–1227 (2013). <https://doi.org/10.1109/JSEN.2012.2228016>
2. Ohno, K., Ito, M., Ichihara, M., Ito, M.: Molecular hydrogen as an emerging therapeutic medical gas for neurodegenerative and other diseases. *Oxid. Med. Cell. Longev.* **2012** (2012). <https://doi.org/10.1155/2012/353152>
3. Hayashida, K., et al.: Inhalation of hydrogen gas reduces infarct size in the rat model of myocardial ischemia-reperfusion injury. *Biochem. Biophys. Res. Commun.* **373**, 30–35 (2008). <https://doi.org/10.1016/j.bbrc.2008.05.165>
4. Ohsawa, I., et al.: Hydrogen acts as a therapeutic antioxidant by selectively reducing cytotoxic oxygen radicals. *Nat. Med.* **13**, 688–694 (2007). <https://doi.org/10.1038/nm1577>
5. Ichihara, M., Sobue, S., Ito, M., Hirayama, M., Ohno, K.: Beneficial biological effects and the underlying mechanisms of molecular hydrogen - comprehensive review of 321 original articles. *Med. Gas Res.*, 1–21 (2015). <https://doi.org/10.1186/s13618-015-0035-1>
6. Bhattacharya, S., Panda, A.N., Meyer, H.D.: Multiconfiguration time-dependent Hartree approach to study the OH + H₂ reaction. *J. Chem. Phys.* **132**, 0–8 (2010). <https://doi.org/10.1063/1.3429609>
7. Coutinho, N.D., Aquilanti, V., Sanches-Neto, F.O., Vaz, E.C., Carvalho-Silva, V.H.: *First-principles* molecular dynamics and computed rate constants for the series of OH-HX reactions (X = H or the halogens): *non*-arrhenius kinetics, stereodynamics and quantum tunnel. In: Gervasi, O., et al. (eds.) ICCSA 2018. LNCS, vol. 10964, pp. 605–623. Springer, Cham (2018). https://doi.org/10.1007/978-3-319-95174-4_47
8. Coutinho, N.D., Aquilanti, V., Silva, V.H.C., Camargo, A.J., Mundim, K.C., De Oliveira, H. C.B.: Stereodirectional origin of anti-arrhenius kinetics for a tetraatomic hydrogen exchange reaction: born-oppenheimer molecular dynamics for OH + HBr. *J. Phys. Chem. A* **120**, 5408–5417 (2016). <https://doi.org/10.1021/acs.jpca.6b03958>

9. Panarese, A., Longo, S.: Monte Carlo calculation of the translational relaxation of superthermal H atoms in thermal H₂ gas. *Astrophys. J.* (2012). <https://doi.org/10.1088/0004-637X/749/1/23>
10. Nakayama, M., et al.: Novel haemodialysis (HD) treatment employing molecular hydrogen (H₂)-enriched dialysis solution improves prognosis of chronic dialysis patients: a prospective observational study. *Sci. Rep.* **8**, 1–10 (2018). <https://doi.org/10.1038/s41598-017-18537-x>
11. Nakashima-Kamimura, N., Mori, T., Ohsawa, I., Asoh, S., Ohta, S.: Molecular hydrogen alleviates nephrotoxicity induced by an anti-cancer drug cisplatin without compromising anti-tumor activity in mice. *Cancer Chemother. Pharmacol.* **64**, 753–761 (2009). <https://doi.org/10.1007/s00280-008-0924-2>
12. Dole, M., Wilson, F.R., Fife, W.P.: Hyperbaric hydrogen therapy: a possible treatment for cancer. *Science* **190**, 152–154 (1975). <https://doi.org/10.1126/SCIENCE.1166304>
13. Iuchi, K., et al.: Molecular hydrogen regulates gene expression by modifying the free radical chain reaction-dependent generation of oxidized phospholipid mediators. *Sci. Rep.* **6**, 1–12 (2016). <https://doi.org/10.1038/srep18971>
14. Sobue, S., et al.: Simultaneous oral and inhalational intake of molecular hydrogen additively suppresses signaling pathways in rodents. *Mol. Cell. Biochem.* **403**, 231–241 (2015). <https://doi.org/10.1007/s11010-015-2353-y>
15. Ostojic, S.M.: Molecular hydrogen: an inert gas turns clinically effective. *Ann. Med.* **47**, 301–304 (2015). <https://doi.org/10.3109/07853890.2015.1034765>
16. Huang, C.S., Kawamura, T., Toyoda, Y., Nakao, A.: Recent advances in hydrogen research as a therapeutic medical gas. *Free Radical Res.* **44**, 971–982 (2010). <https://doi.org/10.3109/10715762.2010.500328>
17. Imamura, K., Kimura, K., Fujie, S., Kobayashi, H.: Hydrogen generation from water using Si nanopowder fabricated from swarf. *J. Nanopart. Res.* **18**, 1–7 (2016). <https://doi.org/10.1007/s11051-016-3418-x>
18. Lam, K.Y., Davidson, D.F., Hanson, R.K.: A shock tube study of H₂ + OH → H₂O + H using OH laser absorption. *Int. J. Chem. Kinet.* **45**, 363–373 (2013). <https://doi.org/10.1002/kin.20771>
19. Nguyen, T.L., Stanton, J.F., Barker, J.R.: Ab initio reaction rate constants computed using semiclassical transition-state theory: HO + H₂ → H₂O + H and isotopologues. *J. Phys. Chem. A* **115**, 5118–5126 (2011). <https://doi.org/10.1021/jp2022743>
20. Meisner, J., Kästner, J.: Reaction rates and kinetic isotope effects of H₂ + OH → H₂O + H. *J. Chem. Phys.* **144** (2016). <https://doi.org/10.1063/1.4948319>
21. Brito, B.G.A., Cândido, L., Teixeira Rabelo, J.N., Hai, G.Q.: Thermodynamic properties of solid molecular hydrogen by path integral Monte Carlo simulations. *Chem. Phys. Lett.* **691**, 330–335 (2018). <https://doi.org/10.1016/j.cplett.2017.11.043>
22. Liu, Q., Liu, B., Zhang, Q., Gao, J., Ma, J.: A low-cost, high-efficiency and durable homogeneous system for molecular hydrogen. *Mater. Lett.* **221**, 46–50 (2018). <https://doi.org/10.1016/j.matlet.2018.03.072>
23. Scholes, G.: The radiation chemistry of aqueous solutions of nucleic acids and nucleoproteins. *Prog. Biophys. Mol. Biol.* **13**, 59–104 (2006). [https://doi.org/10.1016/s0079-6107\(63\)80014-0](https://doi.org/10.1016/s0079-6107(63)80014-0)
24. Spothem-Maurizot, M., Mostafavi, M., Douki, T., Belloni, J.: *Radiation Chemistry: From Basics to Applications in Material and Life Science*. EDP Sciences, Les Ulis Cedex (2008)
25. Olivera, G.H., Galassi, M.E., Rivarola, R.D., Gervais, B., Beuve, M.: Production of HO₂ and O₂ by multiple ionization in water radiolysis by swift carbon ions. *Chem. Phys. Lett.* **410**, 330–334 (2005). <https://doi.org/10.1016/j.cplett.2005.05.057>

26. Gérard, B., Bernard, H.: Water radiolysis under extreme conditions. Application to nuclear industry. In: *Radiation Chemistry: From Basics to Applications in Material and Life Sciences*, pp. 53–64 (2008)
27. Chen, J., Xu, X., Zhang, D.H.: A global potential energy surface for the $\text{H}_2 + \text{OH} \leftrightarrow \text{H}_2\text{O} + \text{H}$ reaction using neural networks. *J. Chem. Phys.* **138** (2013). <https://doi.org/10.1063/1.4801658>
28. Martí, C., Pacifici, L., Laganà, A., Coletti, C.: A quantum-classical study of the $\text{OH} + \text{H}_2$ reactive and inelastic collisions. *Chem. Phys. Lett.* **674**, 103–108 (2017). <https://doi.org/10.1016/j.cplett.2017.02.040>
29. Talukdar, R.K., Gierczak, T., Goldfarb, L., Rudich, Y., Madhava Rao, B.S., Ravishankara, A.R.: Kinetics of hydroxyl radical reactions with isotopically labeled hydrogen. *J. Phys. Chem.* **100**, 3037–3043 (1996). <https://doi.org/10.1021/jp9518724>
30. Orkin, V.L., Kozlov, S.N., Poskrebyshev, G.A., Kurylo, M.J.: Rate constant for the reaction of OH with H_2 between 200 and 480K. *J. Phys. Chem. A* **110**, 6978–6985 (2006). <https://doi.org/10.1021/jp057035b>
31. Kaufman, F., Del Greco, F.P.: Fast reactions of OH radicals. In: *Symposium Combustion*, vol. 9, pp. 659–668 (1963). [https://doi.org/10.1016/S0082-0784\(63\)80074-0](https://doi.org/10.1016/S0082-0784(63)80074-0)
32. Coutinho, N.D., Sanches-Neto, F.O., Carvalho-Silva, V.H., de Oliveira, H.C.B., Ribeiro, L. A., Aquilanti, V.: Kinetics of the $\text{OH} + \text{HCl} \rightarrow \text{H}_2\text{O} + \text{Cl}$ reaction: rate determining roles of stereodynamics and roaming, and of quantum tunnelling. *J. Comput. Chem.* **39**, 2508–2516 (2018). <https://doi.org/10.1002/jcc.25597>
33. Head-Gordon, M., Head-Gordon, T.: Analytic MP2 frequencies without fifth-order storage Theory and application to bifurcated hydrogen bonds in the water hexamer. *Chem. Phys. Lett.* **220**, 122–128 (1994). [https://doi.org/10.1016/0009-2614\(94\)00116-2](https://doi.org/10.1016/0009-2614(94)00116-2)
34. Head-Gordon, M., Maurice, D., Oumi, M.: A perturbative correction to restricted open shell configuration interaction with single substitutions for excited states of radicals. *Chem. Phys. Lett.* **246**, 114–121 (1995). [https://doi.org/10.1016/0009-2614\(95\)01111-L](https://doi.org/10.1016/0009-2614(95)01111-L)
35. Marenich, A.V., Cramer, C.J., Truhlar, D.G.: Universal solvation model based on solute electron density and on a continuum model of the solvent defined by the bulk dielectric constant and atomic surface tensions. *J. Phys. Chem. B.* **113**, 6378–6396 (2009)
36. Aquilanti, V., Coutinho, N.D., Carvalho-Silva, V.H.: Kinetics of low-temperature transitions and reaction rate theory from non-equilibrium distributions. *Philos. Trans. R. Soc. London A* **375**, 20160204 (2017). <https://doi.org/10.1098/rsta.2016.0201>
37. Aquilanti, V., Borges, E.P., Coutinho, N.D., Mundim, K.C., Carvalho-Silva, V.H.: From statistical thermodynamics to molecular kinetics: the change, the chance and the choice. *Rend. Lincei Sci. Fis. e Nat.* **28**, 787–802 (2018). <https://doi.org/10.1007/s12210-018-0749-9>
38. Silva, V.H.C., Aquilanti, V., De Oliveira, H.C.B., Mundim, K.C.: Uniform description of non-Arrhenius temperature dependence of reaction rates, and a heuristic criterion for quantum tunneling vs classical non-extensive distribution. *Chem. Phys. Lett.* **590**, 201–207 (2013). <https://doi.org/10.1016/j.cplett.2013.10.051>
39. Carvalho-Silva, V.H., Aquilanti, V., de Oliveira, H.C.B., Mundim, K.C.: Deformed transition-state theory: deviation from Arrhenius behavior and application to bimolecular hydrogen transfer reaction rates in the tunneling regime. *J. Comput. Chem.* **38**, 178–188 (2017)
40. Christov, S.G.: The characteristic (crossover) temperature in the theory of thermally activated tunneling processes. *Mol. Eng.* **7**, 109–147 (1997). <https://doi.org/10.1023/A:1008274213168>
41. Bell, R.P.: *The Tunnel Effect in Chemistry*. Chapman and Hall, London (1980)

42. Aquilanti, V., Mundim, K.C., Elango, M., Kleijn, S., Kasai, T.: Temperature dependence of chemical and biophysical rate processes: phenomenological approach to deviations from Arrhenius law. *Chem. Phys. Lett.* **498**, 209–213 (2010). <https://doi.org/10.1016/j.cplett.2010.08.035>
43. Nguyen, T.L., Stanton, J.F., Barker, J.R.: A practical implementation of semi-classical transition state theory for polyatomics. *Chem. Phys. Lett.* **499**, 9–15 (2010). <https://doi.org/10.1016/j.cplett.2010.09.015>
44. Atkinson, R., et al.: Evaluated kinetic and photochemical data for atmospheric chemistry: volume I - gas phase reactions of Ox, HOx, NOx and SOx species. *Atmos. Chem. Phys.* **4**, 1461–1738 (2004). <https://doi.org/10.5194/acp-4-1461-2004>
45. Oldenborg, B.C., Loge, G.W., Harradine, D.M., Winn, K.R.: Kinetic study of the OH + H₂ reaction from 800 to 1550 K. *J. Phys. Chem.* **96**, 8426 (1992)
46. Gardiner, W.C. (ed.): *Combustion Chemistry*. Springer-Verlag NY Inc. (1984). <https://doi.org/10.1007/978-1-4684-0186-8>
47. Ravishankara, A.R., Nicovich, J.M., Thompson, R.L., Tully, F.P.: Kinetic study of the reaction of OH with H₂ and D₂ from 250 to 1050K. *J. Phys. Chem.* **85**, 2498–2503 (1981)
48. Marin, T.W., Jonah, C.D., Bartels, D.M.: Reaction of OH* radicals with H₂ in sub-critical water. *Chem. Phys. Lett.* **371**, 144–149 (2003). [https://doi.org/10.1016/S0009-2614\(03\)00064-2](https://doi.org/10.1016/S0009-2614(03)00064-2)
49. Christensen, H., Sehested, K.: Reaction of hydroxyl radicals with hydrogen at elevated temperatures. Determination of the activation energy. *J. Phys. Chem.* **87**, 118–120 (1983). <https://doi.org/10.1021/j100224a027>
50. Schmidt, K.H.: Measurement of the activation energy for the reaction of the hydroxyl radical with hydrogen in aqueous solution. *J. Phys. Chem.* **81**, 1257–1263 (1977). <https://doi.org/10.1021/j100528a008>
51. Santin, L.G., Toledo, E.M., Carvalho-Silva, V.H., Camargo, A.J., Gargano, R., Oliveira, S. S.: Methanol solvation effect on the proton rearrangement of curcumin's enol forms: an ab initio molecular dynamics and electronic structure viewpoint. *J. Phys. Chem. C* **120**, 19923–19931 (2016). <https://doi.org/10.1021/acs.jpcc.6b02393>
52. Machado, D.F.S., et al.: Fully relativistic rovibrational energies and spectroscopic constants of the lowest X:(1)0+g, A':(1)2u, A:(1)1 u, B':(1)0-u and B:(1)0+u states of molecular chlorine. *J. Mol. Model.* **18**, 4343–4348 (2012). <https://doi.org/10.1007/s00894-012-1429-9>
53. Carvalho-Silva, V.H., Coutinho, N.D., Aquilanti, V.: Description of deviations from Arrhenius behavior in chemical kinetics and materials science. In: *AIP Conference Proceedings*, p. 20006. AIP Publishing (2016). <https://doi.org/10.1063/1.4968632>
54. Agreda, N.J.L.: Aquilanti-Mundim deformed Arrhenius model in solid-state reactions: theoretical evaluation using DSC experimental data. *J. Therm. Anal. Calorim.* **126**, 1175–1184 (2016). <https://doi.org/10.1007/s10973-016-5566-8>
55. Romagnoli, É.S., Borsato, D., Silva, L.R.C., Chendynski, L.T., Angilelli, K.G., Canesin, E.A.: Kinetic parameters of the oxidation reaction of commercial biodiesel with natural antioxidant additives. *Ind. Crops Prod.* (2018). <https://doi.org/10.1016/j.indcrop.2018.08.077>
56. Carvalho-Silva, V.H., Coutinho, N.D., Aquilanti, V.: Temperature dependence of rate processes beyond arrhenius and eyring: activation and transitivity. *Front. Chem.* **7**, 380 (2019). <https://doi.org/10.3389/fchem.2019.00380>